

Mechanistic Insights on Azide–Nitrile Cycloadditions: On the Dialkyltin Oxide–Trimethylsilyl Azide Route and a New Vilsmeier–Haack-Type Organocatalyst

David Cantillo,[†] Bernhard Gutmann, and C. Oliver Kappe*

Christian Doppler Laboratory for Microwave Chemistry (CDLMC) and Institute of Chemistry, Karl-Franzens-University Graz, Heinrichstrasse 28, A-8010 Graz, Austria

S Supporting Information

ABSTRACT: The mechanism of the azide–nitrile cycloaddition mediated by the known dialkyltin oxide–trimethylsilyl azide catalyst system has been addressed through DFT calculations. The catalytic cycle for this tin/silicon complex-based mechanism has been thoroughly examined, disclosing the most plausible intermediates and the energetics involved in the rate enhancement. In addition, a new catalyst, 5-azido-1-methyl-3,4-dihydro-2*H*-pyrrolium azide, is presented for the formation of tetrazoles by cycloaddition of sodium azide with organic nitriles under neutral conditions. The efficiency of this organocatalyst, generated in situ from *N*-methyl-2-pyrrolidone (NMP), sodium azide, and trimethylsilyl chloride under reaction conditions, has been examined by preparation of a series of 5-substituted-1*H*-tetrazoles. The desired target structures were obtained in high yields within 15–25 min employing controlled microwave heating. An in depth computational analysis of the proposed catalytic cycle has also been addressed to understand the nature of the rate acceleration. The computed energy barriers have been compared to the dialkyltin oxide–trimethylsilyl azide metal-based catalyst system. Both the tin/silicon species and the new organocatalyst accelerate the azide–nitrile coupling by activating the nitrile substrate. As compared to the dialkyltin oxide–trimethylsilyl azide method, the organocatalytic system presented herein has the advantage of higher reactivity, in situ generation from inexpensive materials, and low toxicity.

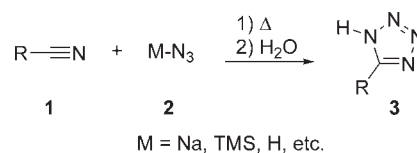


INTRODUCTION

Interest in 5-substituted-1*H*-tetrazoles has increased rapidly over the past few years, in particular due to the value of the tetrazole functionality as a metabolically stable substitute for the carboxylic acid group in biologically active molecules.¹ Apart from their use in medicinal chemistry, tetrazoles have found widespread application in a variety of fields including material science, coordination chemistry, and in organic synthesis as precursors for the preparation of nitrogen-containing heterocycles.²

The usual method for the preparation of 1*H*-tetrazoles of type 3 is the direct cycloaddition of an azide precursor 2 to an organic nitrile 1 in an acidic environment (Scheme 1). Unfortunately, this transformation is very slow, and drastic conditions such as high temperatures and long reaction times, or strong electron-withdrawing substituents on the nitrile counterpart, are needed to achieve efficient conversion to the tetrazole nucleus. A large variety of additives such as Brønsted and Lewis acids,³ or various heterogeneous catalysts⁴ have been reported to accelerate the tetrazole formation. Furthermore, trimethylsilyl,⁵ trialkyltin,⁶ and organoaluminum azides⁷ were introduced as replacements for inorganic azide sources. One of the most common methods to prepare 5-substituted-1*H*-tetrazoles 3 still is the protocol developed by Finnegan and Lofquist in 1958 employing NaN_3 as the azide source in combination with ammonium salts in DMF

Scheme 1. Formation of Tetrazoles from an Organic or Inorganic Azide Source and a Nitrile



or *N*-methylpyrrolidone (NMP) as solvent.^{3a} More recently, a zinc-catalyzed azide–nitrile cycloaddition in water or DMF as solvent was developed by the Sharpless group.⁸

The mechanism of tetrazole formation has been previously investigated through computational methods.⁹ In these studies, stepwise^{9a} and concerted^{9b,c} pathways have been proposed for the cycloaddition step. Noodleman and Sharpless investigated the role of ammonium ion additives on the azide–nitrile reaction^{9c} and, subsequently, the mechanism of activation by zinc(II) salts.¹⁰ In their DFT studies, they concluded that activation of the nitrile substrate, rather than the activation of the azide anion, by zinc(II) is the crucial factor for tetrazole formation.¹⁰

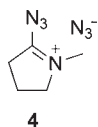
Received: November 5, 2010

Published: March 07, 2011

Apart from the use of ammonium halides or zinc salts as additives/catalysts for the reaction of nitriles with sodium azide, dialkyltin oxides in combination with trimethylsilyl azide (TMSN_3) as comparatively safe azide source have also been employed for tetrazole synthesis.¹¹ Despite the apparent efficiency of the tin-catalyzed tetrazole formation, computational studies regarding the mechanism of activation have not been reported, and, thus, the correct catalytic cycle and the nature of the catalyst is unknown.^{11a}

Herein, we present an in depth computational study on the dialkyltin oxide promoted azide–nitrile cycloaddition, including all the plausible intermediates and saddle points. We compare the energetics of the tin-catalyzed process with those for the uncatalyzed cycloaddition and explain the observed rate improvements in the presence of the tin species. The role of TMSN_3 in the catalytic cycle is elucidated. The results suggest that the catalyst can be recovered from an inorganic azide. Therefore, as confirmed experimentally, stoichiometric amounts of the expensive TMSN_3 precursor can be replaced by catalytic quantities in combination with NaN_3 as an inexpensive stoichiometric reagent.

In the course of these investigations, we encountered a new Lewis acid catalyst for the azide–nitrile cycloaddition without a metal in the structure. This novel organocatalyst¹² is 5-azido-1-methyl-3,4-dihydro-2*H*-pyrrolium azide (**4**), which is generated in situ under the reaction conditions, by simply mixing catalytic amounts of TMSCl with NaN_3 in NMP as solvent. This is the first report on an organocatalyst accelerating the formation of tetrazoles. The new catalyst was tested with a series of nitriles exhibiting high efficiency, superior to that of the tin– TMSN_3 system. The mechanism for the catalytic cycle has been computationally addressed through DFT methods. The calculated energetics for the pyrrolium azide-catalyzed cycloaddition allow a rationalization of the significant rate improvement with respect to both the uncatalyzed azide–nitrile cycloaddition and the tin-promoted reaction.



COMPUTATIONAL METHODS

All of the calculations reported in this work were carried out using the Gaussian 09 package.¹³ The B3LYP¹⁴ density-functional method was selected for all the geometry optimizations and frequency analysis. Key transition structures and substrates were additionally reassessed using the M06¹⁵ density-functional with complete geometry optimization (see the Supporting Information). The M06 functional has been recommended for reactions involving metal atoms.¹⁶ The 6-311G(d,p) basis set was employed for C, H, N, O, and Si atoms, while the Stuttgart–Dresden (SDD),¹⁷ augmented by a set of polarization functions ($\zeta = 0.183$),¹⁸ was used to model the Sn atom. All the geometries were optimized including solvation effects. For this purpose, the SMD¹⁹ solvation method was employed. Because *N*-methyl-2-pyrrolidone (NMP) is not internally stored in the Gaussian solvents list, *N,N*-dimethylacetamide (DMA) was selected for all calculations because of their analogous properties. Frequency calculations at 298.15 K on all the stationary points were carried out at the same level of theory as the geometry optimizations to ascertain the nature of the stationary points. Ground and transition states were characterized by none and one imaginary frequency, respectively.

All of the presented relative energies are free energies at 298.15 K with respect to the reactants. Because the reactions were experimentally carried out at 200 °C, frequency calculations at 473.15 K were also performed for key substrates and transition structures to ensure that the temperature change does not affect the drawn conclusions. The relative free energies at 473.15 K are collected in the Supporting Information. Like in previous studies, acetonitrile was selected as the model substrate for the computation of the reaction energetics. Dimethyltin oxide was selected to model the tin species.²⁰

RESULTS AND DISCUSSION

Uncatalyzed 1,3-Dipolar Cycloaddition. The formation of tetrazoles by reaction of nitriles with azides has been previously studied in detail.⁹ We computed the uncatalyzed reaction of trimethylsilyl azide (TMSN_3) and the azide anion (N_3^-) with acetonitrile at our theoretical level, using the same solvent (DMA) as was used for all modeled catalytic cycles to ensure comparability of the energetics of the different processes.

For the reaction with TMSN_3 (**9**), we took into account the two possible approaches, leading to the 1,5 and the 2,5-regioisomers **11** and **13** (Scheme 2). The calculated transition structures (**10** and **12** in Figure 1) reveal that both reaction channels are synchronous concerted cycloadditions, with energy barriers of 45.3 and 50.2 kcal mol⁻¹, respectively. These high energy barriers are in agreement with the extremely low reaction rates observed when the reaction is carried out without the assistance of any catalyst.^{1,2}

With the azide anion as the dipolar species, the calculated energy barrier for the cycloaddition is 38.2 kcal mol⁻¹ and hence significantly lower than the barrier for the reaction with TMSN_3 . This difference in the reactivity was experimentally corroborated by a reaction of benzonitrile with either NaN_3 or TMSN_3 in NMP as solvent. To a 1 M solution of benzonitrile in NMP was added 2 equiv of NaN_3 or TMSN_3 , and the reaction mixtures were heated at 200 °C in a microwave reactor for 15 min. HPLC–UV analysis revealed low conversions in both cases, but the reaction was significantly slower using TMSN_3 as the azide source as compared to the reaction with NaN_3 (17% and 4% conversions for the reactions with NaN_3 and TMSN_3 , respectively).

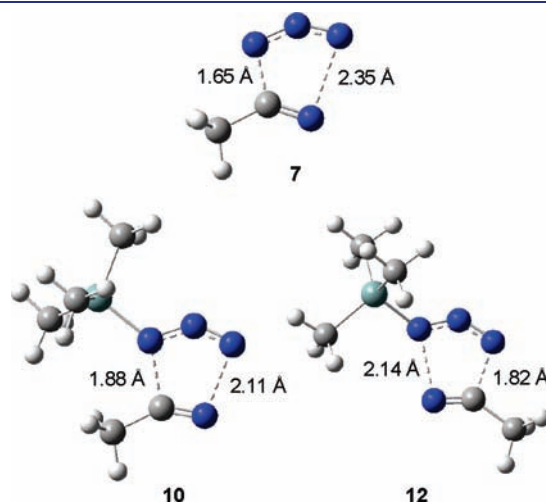
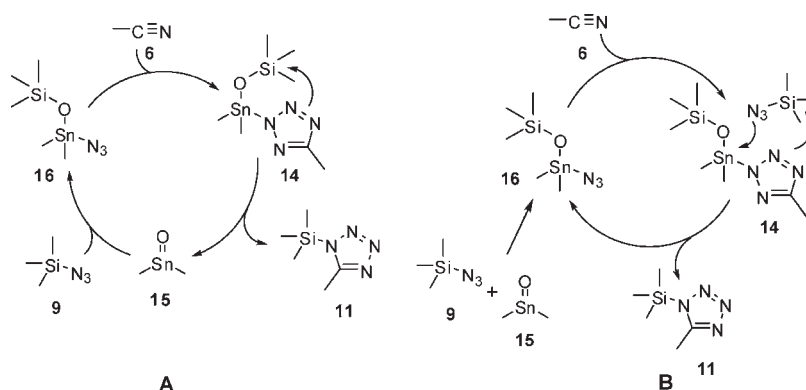
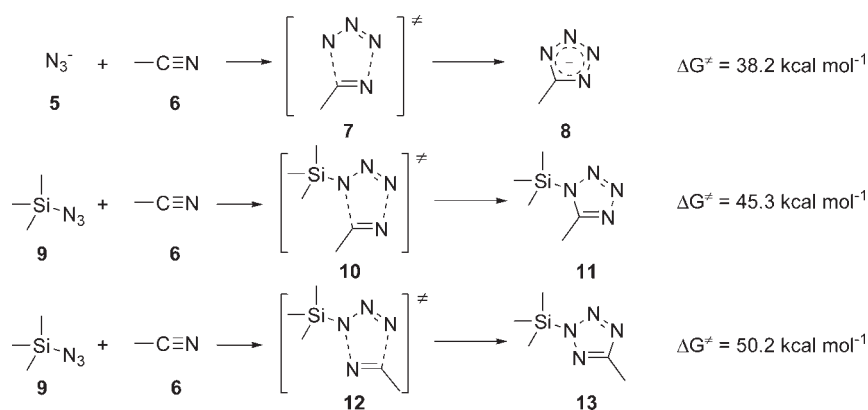


Figure 1. Optimized geometries of the transition structures **7**, **10**, and **12** for the cycloaddition of azide anion and TMSN_3 with acetonitrile (Scheme 2).

Scheme 2. Energy Barriers for the Uncatalyzed Cycloaddition of Azide Anion (5) and TMSN₃ (9) to AcetonitrileFigure 2. Proposed mechanisms for the tin-catalyzed azide-nitrile coupling.^{11a}

It is noteworthy that the addition of the azide anion to the nitrile shows an asynchronous concerted character, while the 1,3-dipolar cycloaddition with TMSN₃ is synchronous. An alternative stepwise mechanism as suggested in a previous study^{9a} could not be located, in agreement with more recently reported B3LYP calculations.^{9b,c} Scheme 2 shows the energy barriers for the 1,3-dipolar cycloadditions of acetonitrile with TMSN₃ and the azide anion.

Tin-Catalyzed 1,3-Dipolar Cycloadditions. Nature of the Catalyst. There are two proposals for the catalytic cycle regarding the tin-promoted reaction of nitriles with TMSN₃.^{11a} Figure 2 depicts the two proposed pathways with acetonitrile (6) as the model substrate and dimethyltin oxide (15) as the catalyst precursor. In catalytic cycle “A”, the dimethyltin oxide (15) is recovered after the cycloaddition process, and hence the tin oxide can be considered as the catalyst. Pathway B, on the other hand, assumes an irreversible formation of complex 16 from dimethyltin oxide and TMSN₃ and it is this complex that has been suggested as the actual catalyst.^{11a} Thus, the catalytic cycle “B” requires a sufficient stability of the intermediate complex 16 with respect to the reactants.

The formation of complex 16 from TMSN₃ and the tin species occurs through the six-membered transition structure 17 (Figure 3). The calculated free energy barrier is only 13.2 kcal mol⁻¹ and thus very low in comparison with the barriers for the uncatalyzed 1,3-dipolar cycloadditions and probably lower than the barrier for any catalyzed azide-nitrile coupling. These energetics point to a very fast formation of the catalyst during the preparation of the reaction

mixture. The reaction is with -48.8 kcal mol⁻¹ extremely exothermic. Complex 16 is therefore particularly stable with respect to the reactants, and the first mechanistic proposal (Figure 2) seems to be improbable, because the recovery of the dialkyltin oxide species would

have an energy penalty of approximately +48 kcal mol⁻¹. Figure 3 shows the optimized geometry for complex 16 and transition structure 17 along with the energy profile for the transformation.

Activation Mechanism for the Tin-Catalyzed Cycloaddition. Once the nature of the catalyst had been addressed, we examined the energetics of the 1,3-dipolar cycloaddition catalyzed by the above-described complex 16. It is essential to take into account the possible activation of both the azide and the nitrile species, as demonstrated by Noodleman and Sharpless in their studies on the activation of the azide-nitrile cycloaddition by zinc(II) salts.¹⁰

In principle, complex 16, where the azide is bound to the tin atom, could react directly with the nitrile via a 1,3-dipolar cycloaddition to afford either of the two regioisomeric complexes 14 or 20 (Figure 4). However, the energy barriers for these transformations, calculated at the B3LYP level, are +49.5 and +44.0 kcal mol⁻¹ (with respect to the free energy of the complex 16) for the 1,5 and the 2,5 approaches, respectively (Figure 4), and hence are similar to those calculated for the uncatalyzed reactions. Therefore, this mechanism cannot explain the observed acceleration of the reaction in the presence of the tin species.

On the other hand, the nitrile carbon could be activated for the cycloaddition if the nitrogen approaches the tin atom in complex **16**. Thus, the addition of complex **16** to acetonitrile to afford complex **20** could take place via a stepwise process (Figure 6). The first step involves the attack of the acetonitrile nitrogen to the acidic tin atom and bonding of the azide to the nitrile carbon. This process occurs through transition structure **21** with a relative free energy of $+32.8$ kcal mol⁻¹ (Figure 6) and leads to the open-chain intermediate **22**. The process is endothermic with an energy penalty of $+21.8$ kcal mol⁻¹. An IRC calculation of the transition state **21** shows that, previous to the addition of the azide anion to the nitrile carbon, an azide–nitrile ligand exchange with a very small barrier takes place at the tin center (see the Supporting Information). The subsequent ring-closing process, through the transition state **23**, has an energy barrier of 11.0 kcal mol⁻¹ with respect to the intermediate **22**. The barrier with respect to the reactants (complex **16** and acetonitrile) is

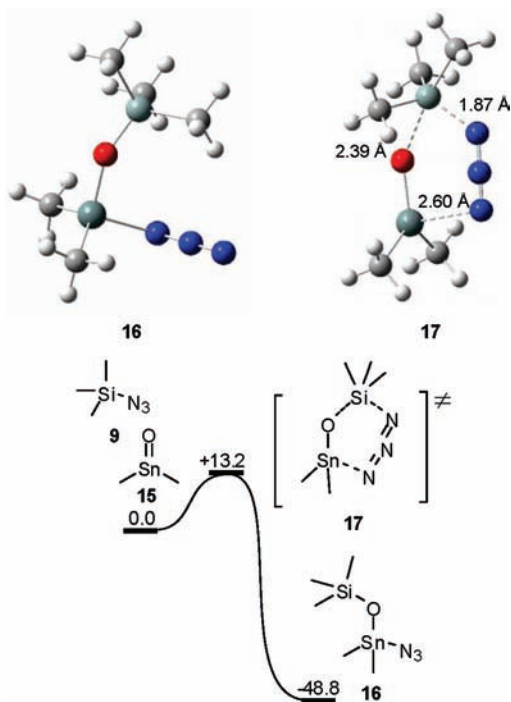


Figure 3. Optimized geometry of the transition structure **17** and the resulting complex **16** and the energy profile for the transformation.

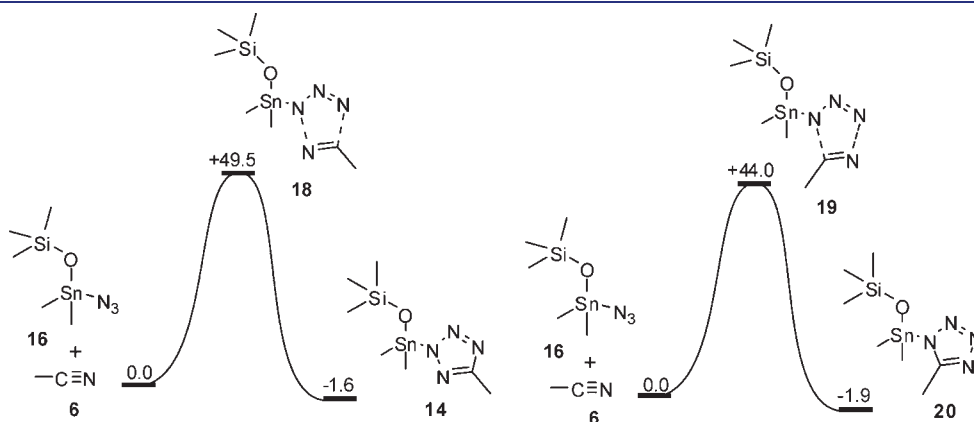


Figure 4. Energetics for the cycloaddition of complex **16** to acetonitrile (**6**). Transition state geometries are shown in Figure 5.

exactly the same as the energy barrier for the first reaction step (Figure 6). The energy of activation for this stepwise reaction with a prior activation of the nitrile is hence significantly lower than that for a direct addition of the azide counterpart of complex **16**. The change in the free energy for the overall process is exothermic by 1.9 kcal mol⁻¹.

The energy of activation for this stepwise process is lower than that for the uncatalyzed reactions by more than 5 kcal mol⁻¹. The crucial role of the tin apparently is the activation of the nitrile molecule, rather than of the azide species, in the same manner as previously reported for the zinc(II)-catalyzed reaction.¹⁰

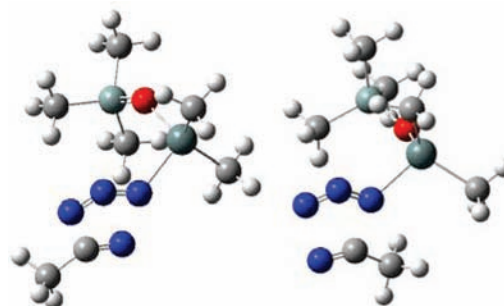


Figure 5. Optimized geometries for the transition structures **18** and **19** leading to complexes **14** and **20** through a direct 1,3-dipolar cycloaddition of complex **16** to acetonitrile (**6**).

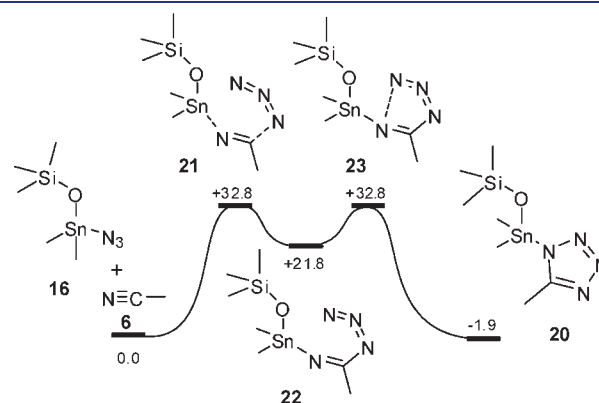


Figure 6. Energy profile for the stepwise process with a prior activation of acetonitrile (**6**) by complex **16**.

Catalyst Recovery. The formation of complex **20** via a stepwise mechanism explains the experimentally observed acceleration of the reaction in the presence of the tin catalyst. To complete the catalytic cycle, we have also investigated the recovery of the catalyst by means of the reaction of **20** with a second TMSN_3 molecule.

The TMS exchange between the azide and one of the tetrazole nitrogens could take place by a concerted process through the transition structure **24** (Figure 7), as suggested by Wittenberg

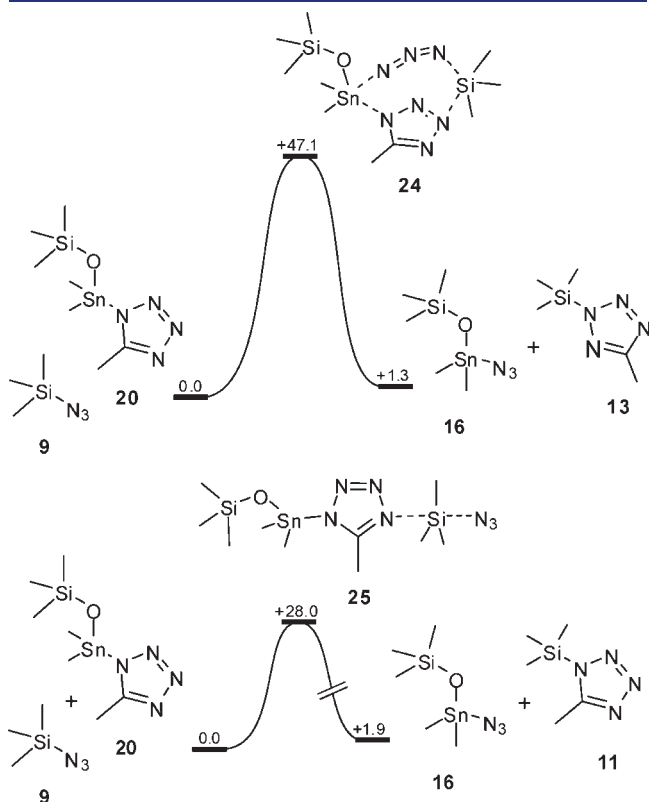


Figure 7. Energy barriers for the recovery of complex **16** through a nucleophilic substitution at the silicon atom.

and Donner.^{11a} The reaction involves the binding of the terminal azide nitrogen in **9** to the tin center and a simultaneous displacement of the proximal azide nitrogen from the TMS group by the tetrazole. In the corresponding transition structure of this pathway (**24**), the silicon atom has the nucleophile and the leaving group on the same side. The calculated energy barrier for this mechanism is $+47.1 \text{ kcal mol}^{-1}$ and hence even higher than the barrier for the uncatalyzed 1,3-dipolar cycloaddition.

An obvious alternative is a simple $\text{S}_{\text{N}}2$ reaction of nitrogen 4 in complex **20** with the silicon atom of the TMSN_3 (**9**). The transition structure (**25**) has a relative energy of only $28.0 \text{ kcal mol}^{-1}$ and regenerates complex **16** and affords *N*-(trimethylsilyl)tetrazole (**11**) after a fast ligand exchange at the tin atom with the azide anion. This ligand exchange is expected to take place without a perceptible energy barrier (Figure 7).

Reaction with Catalytic Amounts of TMSN_3 and NaN_3 as the Stoichiometric Reagent. For the tin-promoted azide–nitrile cycloaddition, TMSN_3 plays two crucial roles in the catalytic cycle. On the one hand, it forms the catalytically active reaction complex **16** from dialkyltin oxide **15** in a highly exothermic reaction, and, on the other hand, it releases *N*-(trimethylsilyl)tetrazole (**11**) from complex **20** and recovers the catalyst through a low energy TMS exchange reaction between the azide and the tetrazole (Figure 7).

The above-mentioned energy barrier for the TMS exchange between the azide and the tetrazole nitrogen (Figure 7) is small in comparison to that for the cycloaddition processes. Therefore, this reaction will be fast under the reaction conditions usually employed for the synthesis of tetrazoles. However, TMSN_3 in turn may be regenerated by an exchange of the tetrazole moiety in *N*-(trimethylsilyl)tetrazole (**11**) by an azide anion derived from an azide source such as NaN_3 . This reaction can take place either on the 1,5 (**11**) or on the 2,5-regioisomer (**13**). The $\text{S}_{\text{N}}2$ reactions with the azide anion as the nucleophile and the tetrazolate as the leaving group proceed via transition states **26** and **27**. The barriers were calculated at the B3LYP level to be 9.0 and $6.6 \text{ kcal mol}^{-1}$, respectively, for the 1,5- and 2,5-isomers (Figure 8).

The azide anion (**5**) could also directly attack the tin atom in the intermediate complex **20**, thus regenerating complex **16** and

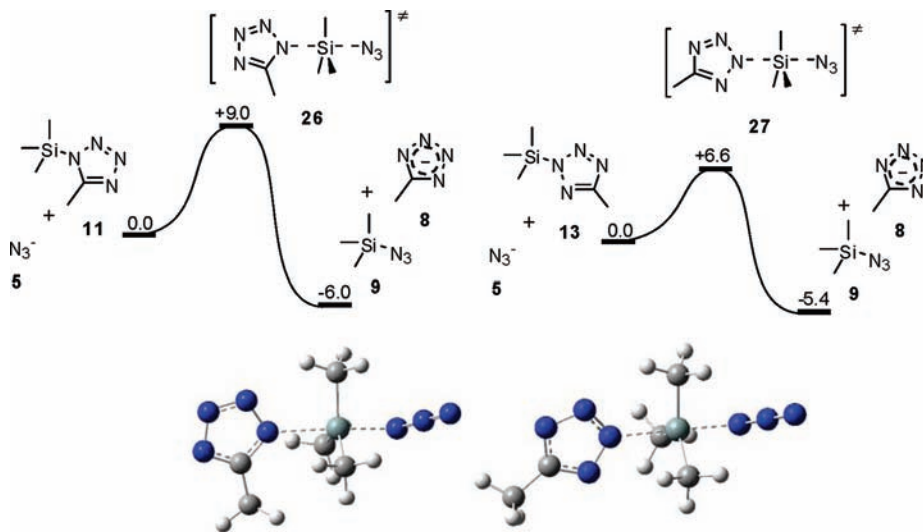


Figure 8. Relative energies and optimized geometries for the transition structures for the TMS exchange between the *N*-(trimethylsilyl)-tetrazoles **11** and **13** and an azide anion, leading to the recovery of the TMSN_3 (**9**).

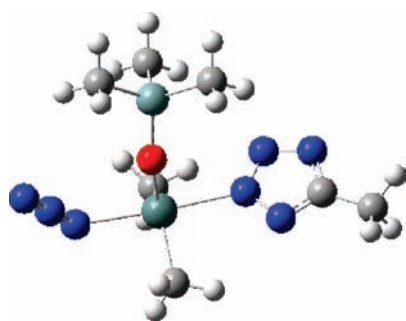
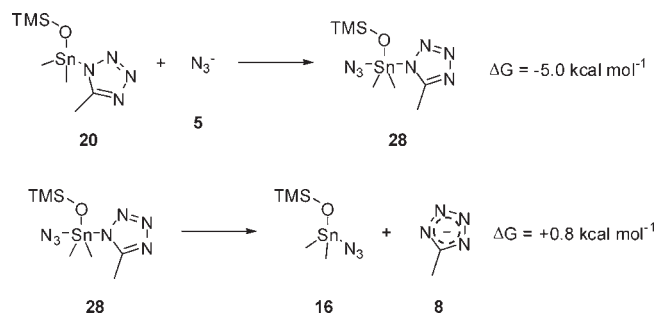


Figure 9. Stable complex resulting from the approach of azide anion (5) to the tin atom in complex 20.

Scheme 3



releasing the tetrazolate anion (8) without the need of a second molecule of TMSN_3 (9) for the recovery of the catalyst. Interestingly, attempts to locate the transition structure for this transformation resulted in a stable pentacoordinated complex (28) (Scheme 3), in which both the azide and the tetrazolate anion remain bonded to the tin atom. The formation of complex 28 is exothermic by $5.0 \text{ kcal mol}^{-1}$. No energy barrier was detected for the approach of the azide ion to the tin atom. The release of the tetrazolate from 28 to recover complex 16 is slightly endothermic ($0.8 \text{ kcal mol}^{-1}$). This means that the catalyst could be also recovered from 20 by a direct nucleophilic substitution of the azide anion at the tin atom (Figure 9).

The above calculations suggest a new catalytic picture (Figure 10). First, the cycle involves the 1,3-dipolar cycloaddition of complex 16 to the nitrile described in Figure 6. Next, the catalyst 16 is recovered from 20 and an azide source (5). Hence, stoichiometric amounts of the expensive TMSN_3 can be replaced by stoichiometric amounts of inexpensive NaN_3 and catalytic amounts of TMSN_3 or even TMSCl (which will readily afford TMSN_3 in the presence of the azide ion).

New Catalytic Picture – Experimental Demonstration. To experimentally corroborate the new and advantageous reaction conditions suggested by our theoretical study, employing only catalytic amounts of TMSN_3 (or TMSCl) and stoichiometric amounts of NaN_3 , we carried out the reaction of benzonitrile and NaN_3 in different solvents employing varying amounts of dibutyltin oxide and TMSCl (up to 0.15 equiv) (Table 1). All the reactions were conducted using controlled microwave heating at 200°C for 15 min.

Low conversions were obtained after 15 min at 200°C in the absence of a TMS species, ranging from conversions below 1% in toluene to 17% in NMP, irrespective of whether tin oxide was present in the reaction mixture or not. As anticipated, the

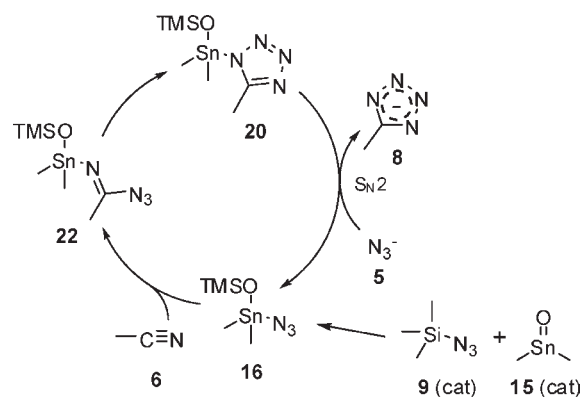


Figure 10. New catalytic cycle deduced from DFT calculations. Only catalytic amounts of TMSN_3 (9) and dialkyltin oxide (15) are needed. The catalyst tin complex 16 is recovered during the transformation by an azide source (5).

Table 1. Conversions Achieved for the Reaction of Benzonitrile and NaN_3 with Different Amounts of TMSCl and Bu_2SnO at 200°C for 15 min^a

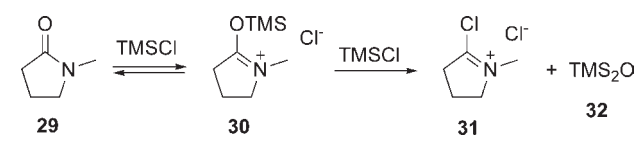
%TMSCl/%Bu ₂ SnO:	conversion ^b					
	0/0	0/15	15/15	15/10	15/5	15/0
toluene	<1%	<1%	13%	27%	43%	<1%
DMA	13%	16%	51%	60%	54%	27%
DMF	11%	11%	40%	48%	44%	35%
NMP	17%	17%	60%	66%	76%	85%

^a For a graphical representation, see Figure S1 in the Supporting Information. ^b HPLC-UV conversion at 190 nm.

addition of substoichiometric amounts of TMSCl increased the reaction rate greatly in all tested solvents. Essentially equal results were obtained employing (the far more expensive) TMSN_3 instead of TMSCl as additive. It is interesting to note that superior conversions were achieved with an excess of TMSCl over dibutyltin oxide. Employing a constant amount of TMSCl in toluene, DMA, or DMF as solvent, the reaction rate increased with an increasing $\text{TMSCl}/\text{Bu}_2\text{SnO}$ ratio, passed through a maximum, and then decreased sharply when the amount of Bu_2SnO was further reduced. Because the catalytically active complex 16 can be recovered by a direct displacement of the tetrazolate 8 from intermediate 20 by an azide anion, an excess of TMSCl (or TMSN_3) ought not to be required, and we attribute this observed acceleration to an assistance of the TMS species in the release of the tetrazole anion from complex 28.

Overall, the results obtained in toluene, DMF, and DMA are in agreement with the new catalytic picture in which stoichiometric amounts of NaN_3 can be used to form 1*H*-tetrazoles and only catalytic amounts of the expensive tin and TMS species are required to catalyze the transformation. However, the reaction carried out in NMP did not behave as expected. Surprisingly, the reaction rate increased steadily with decreasing amounts of dibutyltin oxide. Indeed, the “catalyst-free” reaction was remarkably efficient. With 15% of TMSCl , but without any tin oxide as additive, a conversion of 85% was achieved after 15 min at 200°C . With increasing amounts of dibutyltin oxide in the reaction mixture, however, the reaction rate is reduced and approaches those observed in DMA or DMF as solvent under otherwise identical conditions. These observations are especially

Scheme 4



intriguing considering the very similar physical properties of the solvents DMA, DMF, and NMP, suggesting that the NMP/TMSCl system catalyzes the tetrazole formation in some specific way. Addition of the dialkyltin oxide will form the stable complex 16 and will sequester TMSCl in the medium and slow the reaction rate.

Literature data suggest that cyclic amide structures such as NMP (29) in solution are in equilibrium with *O*-trimethylsilyl salts (30) when electrophilic reagents such as TMSCl or TMSN₃ (Scheme 4) are added.²¹ This salt will react with a second equivalent of TMSCl to afford the Vilsmeier-Haack-type reagent 5-chloro-1-methyl-3,4-dihydro-2H-pyrrolium chloride (31) and hexamethyldisiloxane (32) (Scheme 4).

With the aim to experimentally corroborate this hypothesis, we mixed equimolar amounts of NMP and TMSCl and heated the mixture at 200 °C for 5 min to reproduce the reaction conditions. The reaction mixture was subsequently cooled, and diethyl ether was added slowly to precipitate a white hygroscopic crystalline solid. The structure of the precipitate was assigned to 5-chloro-1-methyl-3,4-dihydro-2H-pyrrolium chloride (31) by means of ¹H and ¹³C NMR spectroscopy (see the Supporting Information). To further confirm the structure of the isolated product, we carried out the reaction of NMP with oxalyl chloride, a reagent known to provide Vilsmeier-Haack-type intermediates upon reaction with NMP.²² Thus, to a cooled solution of NMP in diethyl ether was slowly added a solution of oxalyl chloride in diethyl ether. Immediately, a white solid crystallized from the reaction mixture. The ¹H NMR spectra of this strongly hygroscopic compound confirmed the proposed structure for dihydropyrrolium chloride 31 (Figure 11). Indeed, the pure isolated compound 31, obtained by the known reaction of NMP and oxalyl chloride,²² exhibited a marked catalytic activity for the 1,3 dipolar-cycloaddition. Compound 31 added in catalytic amounts (0.15 equiv) to benzonitrile and NaN₃ in NMP as solvent resulted in a >90% conversion after heating the mixture at 200 °C for 15 min.

An excess of NaN₃ in the mixture of TMSCl in NMP presumably will displace the chlorine atoms in 31 to afford 5-azido-1-methyl-3,4-dihydro-2H-pyrrolium azide (4) (Scheme 5). Similar anion displacements with NaN₃ have been previously described for Vilsmeier-Haack-type structures.²³

Ionic dihydropyrrolium azide 4, which is expected to exist in equilibrium with its covalently bonded isomeric equivalent 4', exhibits a pronounced positive charge at carbon C-2, and a marked Lewis acid character and thus could participate in the azide-nitrile 1,3-dipolar cycloaddition in an analogous fashion as other Lewis acids such as zinc(II) salts or the tin species (Figure 12).

Attempts to prepare and isolate 5-azido-1-methyl-3,4-dihydro-2H-pyrrolium azide (4) by direct reaction of NMP and TMSN₃ in an analogous manner as described for dihydropyrrolium chloride 31 were unsuccessful. When heating a NMP-TMSN₃ mixture, 4 could not be detected by NMR analysis, and, as emphasized above, the uncatalyzed reaction of benzonitrile with

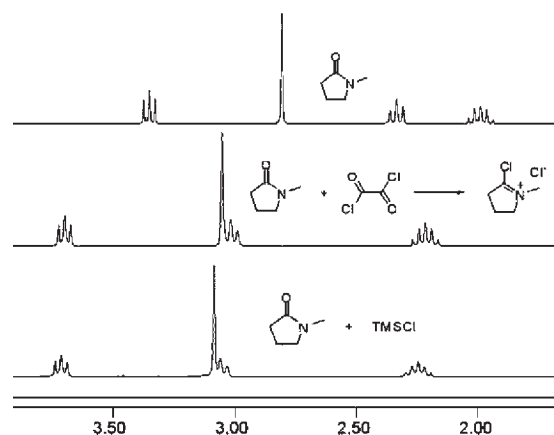


Figure 11. ¹H NMR spectra of NMP (top), the Vilsmeier-Haack-type structure 31 obtained through reaction of NMP with oxalyl chloride (middle), and the solid obtained by treatment of NMP with TMSCl (bottom).

Scheme 5

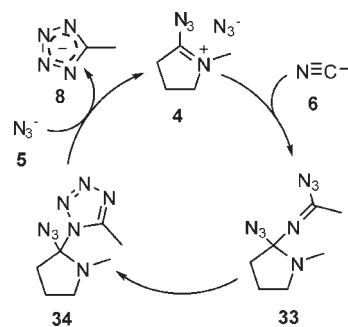
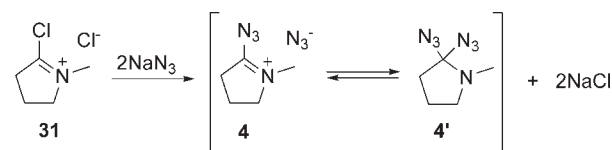


Figure 12. Proposed catalytic cycle for the tetrazole formation assuming species 4 as catalyst.

TMSN₃ in NMP as solvent was even slower than the uncatalyzed reaction with NaN₃. However, with NaN₃ as reagent and substoichiometric amounts of TMSN₃, the achieved conversions were excellent. This suggests that the formation of dihydropyrrolium azide 4 from TMSN₃ and NMP requires the presence of the azide anion, while the formation of dihydropyrrolium chloride 31, which can be considered as a precatalyst, has no need of assistance.

In principle, solvents such as DMA and DMF should exhibit a behavior similar to that NMP when carrying out reactions in those solvents. However, excellent conversions were only achieved when using the cyclic amide NMP, presumably due to the higher nucleophilicity of this solvent (Table 1).²¹

Tetrazole Formation Mechanism Assisted by Dihydropyrrolium Azide 4. The new catalyst for the tetrazole formation has demonstrated an experimental efficiency superior to that observed for the tin species under identical reaction conditions.

Scheme 6

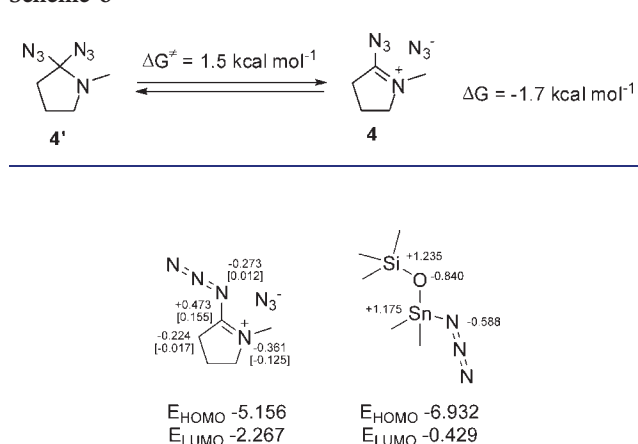


Figure 13. Charge distribution and orbital energies (eV) for the HOMO and LUMO (coefficients in brackets) in dihydropyrrolium azide 4 (left) and tin complex 16 (right).

The theoretical calculations of the energetics involved during the transformation of the nitrile to the tetrazole, as outlined in Figure 12, can help to understand the nature of the catalyst and the mechanism of acceleration. Thus, we calculated at the same level of theory as used for the calculations above the 1,3-dipolar cycloaddition assisted by structure 4 as Lewis acid.

The catalyst is expected to be in equilibrium between the covalently bonded geminal diazide species (4'), and the ionic pair 4. The geometries of both structures were optimized, as well as the transition structure for the interconversion of the two species. As expected, the energy barrier for the conversion is very low (1.5 kcal mol⁻¹), which points to a very fast equilibrium. The ionic structure (4) is more stable than the covalently bonded structure (4') by 1.7 kcal mol⁻¹ (Scheme 6). Therefore, the ionic structure free energy will be used as the reference for the calculations of the energy barriers.

The charge distribution in dihydropyrrolium azide 4 reveals a pronounced positive charge at the C-2 atom (Figure 13). This suggests that the carbon could have a marked acidic character. The Lewis acidity of this structure, or its ability to gain electronic density, can be related to the LUMO energy. The lower the LUMO energy, the larger will be the ability to gain electronic density. The analysis of the molecular orbitals (Figure 13) shows a lower LUMO energy for dihydropyrrolium azide 4 in comparison to the tin complex 16. In addition, the coefficients show that the LUMO is mainly located at the carbon atom adjacent to the dihydropyrrolium nitrogen, indicating that this atom will act as the Lewis acid center.

To corroborate this hypothesis, we have calculated the energetics involved in the catalytic cycle depicted in Figure 12. The process starts with the approach of the nitrile to the positively charged atom of the ionic form of the dihydropyrrolium azide 4. This process can occur without appreciable energy barrier. The approach of the azide to the carbon atom of the activated nitrile is expected to have a very small energy barrier, similar to that found for the corresponding reaction of the tin-catalyzed process (Figure 6). However, attempts to locate this saddle point were unsuccessful. In all cases, the carbon–nitrogen bond was formed during the geometry optimization process. To further confirm the lack of a barrier for this process, we calculated the approach of

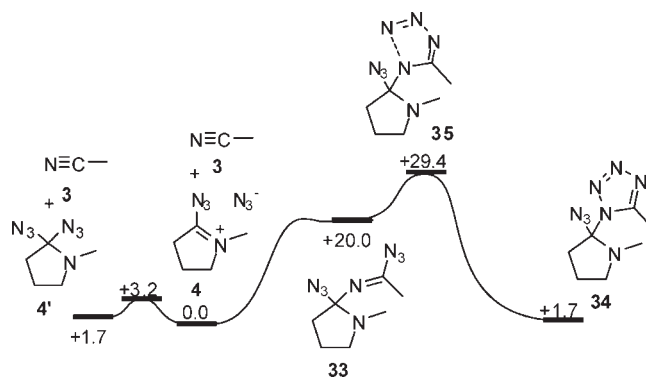


Figure 14. Energy profile for the tetrazole formation assisted by the organocatalyst 4.

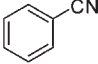
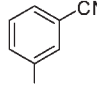
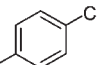
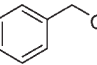
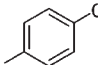
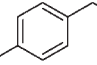
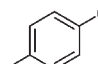
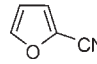
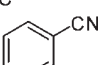
the azide to the positively charged atom, with intervals of 0.05 Å, optimizing the geometry for each step. This C–N bond length scan does not reveal any energy maximum (see the Supporting Information). In contrast, for the tin-catalyzed nitrile–azide bond formation, this method succeeded in locating the transition structure. Although the above-mentioned bond length scan does not reveal an energy barrier for the formation of 33, because the reaction is endothermic, a negligible energy barrier could be expected for the process. Presumably, the above-mentioned higher Lewis acid character of the positively charged carbon atom of dihydropyrrolium azide 4 in comparison with that of the tin atom in complex 16 makes the formation of the intermediate 33 (Figure 14) a very fast process.

The overall barrier for the formation of the tetrazole ring is +29.4 kcal mol⁻¹ and hence lower than the barrier of the tin-catalyzed pathway by more than 3 kcal mol⁻¹. This explains the higher reaction rate of the reaction in NMP with catalytic amounts of TMSCl in the absence of tin oxide as compared to the dialkyltin oxide/TMSCl catalyzed reaction under otherwise identical conditions. Because the formation of tin complex 16 is a very fast and an irreversible process, the addition of dialkyltin oxide to the NMP–TMSCl mixture reduces the amount of TMSCl available to generate the organocatalyst 4 and consequently decreases the reaction rate for the tetrazole formation to the rate of the less efficient process catalyzed by complex 16 (Table 1).

After the 1,3-dipolar cycloaddition, the organocatalyst is recovered through a nucleophilic substitution at the carbon. This is expected to be a S_N1 process, because the positive charge on the carbon would be stabilized by the adjacent nitrogen and the azide group. After the dissociation of the tetrazolate anion, a new azide anion provided by the azide source (NaN₃) would regenerate catalyst 4. The calculated energy barrier for the dissociation of the tetrazole–catalyst complex is with 6.0 kcal mol⁻¹ (Scheme 7) similar to that calculated for the recovery of TMSN₃ from TMS tetrazolate by nuclear substitutions at the silicon atom (Figure 8).

Scope of the New Organocatalyst. The surprisingly high efficiency of the organocatalyst 4 in accelerating the formation of tetrazoles prompted us to optimize the reaction conditions and to explore the preparative scope of the transformation. The optimization of the reaction conditions was carried out using benzonitrile as a model substrate, 0.15 equiv of TMSCl, and 1.2 equiv of NaN₃. A set of optimization studies involving different temperatures and reaction times was performed under microwave

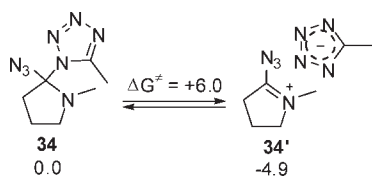
Table 2. Preparation of Tetrazoles 3 in the Presence of Organocatalyst 4 (Scheme 1, M = Na)^a

	Substrate	Time (min)	Yield (%) ^b	Substrate	Time (min)	Yield (%) ^b	
3a		15	79	3f		15	96
3b		15	95	3g		20	96
3c		20	82	3h		25	86
3d		15	93	3i		15	92
3e		15	87				

^a Reaction conditions: 1 mmol of nitrile, 1.2 mmol of NaN₃, 0.15 mmol of TMSCl, 1.0 mL of NMP. Single-mode microwave heating at 220 °C.

^b Isolated yield.

Scheme 7



conditions with the best set of conditions found to be 15 min of heating at 220 °C (Figure S2 in the Supporting Information).

To assess the scope and limitations of the cycloaddition catalyzed by 4, we tested a series of nitriles with both electron-withdrawing and electron-donating substituents. The heating times for these cycloadditions ranged from 15 to 25 min, depending on the reactivity of the substrate. Isolated product yields were >80% for all studied examples (Table 2). The results presented herein represent a significant improvement compared to previously described methods for azide–nitrile cycloadditions using catalysts based on tin or zinc metals. In addition, the present organocatalyst has the advantage of low price, ease of handling, and low toxicity. As no acid is involved, the conditions can be regarded as safe because no hydrogen azide (HN₃) will be liberated.²⁴

CONCLUSIONS

In summary, we have presented an in depth analysis of the mechanism of the tin-catalyzed tetrazole formation. A DFT analysis of most of the plausible reaction channels allowed us to ascertain the nature of the intermediates involved in the catalytic cycle and to determine the structure of the organotin compound 16, which acts as the catalyst. Because of the high exothermicity of the formation of structure 16, $-48.8 \text{ kcal mol}^{-1}$, it presents an irreversible character, and thus the dialkyltin oxide species (15) cannot be recovered during the catalytic cycle.

The calculation of the energy barriers for the uncatalyzed 1,3-dipolar cycloadditions of TMSN₃ (9) and of the azide anion (5), 45.3 (for the 1,5-regiochemistry) and 38.2 kcal mol⁻¹, respectively, was performed at the same level of theory as the catalytic

cycles to guarantee comparability. If the tin atom in complex 16 is supposed to activate the azide, the calculated barriers are 49.5 and 44.0 kcal mol⁻¹ for the 1,5- and 2,5- approaches, respectively (Figure 4). These energetics are analogous to the uncatalyzed reactions, and therefore this pathway cannot explain the observed rate acceleration. However, if the nitrile is the activated species, the overall energy barrier of the process is 32.8 kcal mol⁻¹, more than 5 kcal mol⁻¹ lower than that for the nitrile–azide anion reaction, and more than 10 kcal mol⁻¹ lower than the barrier computed for the TMSN₃–nitrile cycloaddition. Thus, in agreement with previous studies on the tetrazole formation in the presence of Lewis acids,¹⁰ the nitrile activation is most likely responsible for the experimentally observed rate acceleration.

The analysis of the theoretical calculations allowed us to suggest new catalytic conditions. Thus, it is possible to replace the expensive TMSN₃ reagent by stoichiometric amounts of NaN₃ employing only catalytic amounts of TMSCl. The tetrazolate anion (8) can be released from the intermediate complex 20, likely through a ligand exchange with the azide anion. This new catalytic picture, proposed by means of theoretical calculations, has been corroborated experimentally.

In this work, we have also suggested a new organocatalyst for the azide–nitrile cycloaddition. This catalyst, 5-azido-1-methyl-3,4-dihydro-2H-pyrrolium azide (4), is presumably formed by addition of TMSCl to the reaction mixture when NMP is used as solvent. The structure of the dihydropyrrolium chloride precursor 31 has been confirmed by comparison of the NMR spectra with the Vilsmeier–Haack reagent obtained by reaction of NMP with oxalyl chloride. Moreover, the isolated product was successfully used as catalyst for the reaction of benzonitrile with NaN₃. The efficiency of the new catalyst has been investigated with a collection of organic nitriles, decorated with electron-withdrawing and electron-donor groups. Excellent yields were obtained in all of the studied cases.

To further comprehend the nature of the new organocatalyst and its high efficiency, we have also calculated the energetics involved in the proposed catalytic cycle for the azide–nitrile cycloaddition activated by this Vilsmeier–Haack-type compound. The overall energy barrier for the catalyzed pathway was calculated to be

Table 3. Summary of Experimental Conversions and Computed Energy Barriers for the Cycloaddition of Benzonitrile with NaN_3

catalyst	conversion ^a	key TS	activation barrier (kcal mol ⁻¹) ^b
none ^c	4%	10	45.3
none	17%	7	38.2
NMP–TMSCl–Bu ₂ SnO	60%	21, 23	32.8
NMP–TMSCl	85%	35	29.4

^a In NMP, at 200 °C for 15 min. ^b At the B3LYP/SSD,6-311G(d,p) level. ^c TMSN₃ as substrate.

+29.4 kcal mol⁻¹, more than 3 kcal mol⁻¹ lower than the barrier for the tin-catalyzed mechanism, and hence explaining the observed rate enhancement when using the NMP–TMSCl reaction mixture in comparison to the NMP–TMSCl–Bu₂SnO catalytic mixture. The above energy barriers are in qualitative agreement with the observed conversions in all of the reactions experimentally performed, as summarized in Table 3.

Finally, we note that the reported organocatalysts **4** and **31** could be useful in a wide range of reactions generally catalyzed by Lewis acids, taking into account its marked electrophilic character, and the advantages derived from its simple preparation and low toxicity in comparison with metal-based catalysts.

EXPERIMENTAL SECTION

General Remarks. ¹H NMR spectra were recorded on a Bruker 300 MHz instrument. ¹³C NMR spectra were recorded on the same instrument at 75 MHz. Chemical shifts (δ) are expressed in ppm downfield from TMS as internal standard. The letters s, d, t, q, and m are used to indicate singlet, doublet, triplet, quadruplet, and multiplet, respectively. Analytical HPLC (Shimadzu LC20) analysis was carried out on a C18 reversed-phase (RP) analytical column (150 × 4.6 mm, particle size 5 mm) at 25 °C using a mobile phase A (water/acetonitrile 90:10 (v/v) + 0.1% TFA) and B (MeCN + 0.1% TFA) at a flow rate of 1.0 mL min⁻¹. The following gradient was applied: linear increase from solution 30% B to 100% B in 8 min, hold at 100% solution B for 2 min. Melting points were determined on a Stuart SMP3 melting point apparatus. All anhydrous solvents (stored over molecular sieves) and chemicals were obtained from standard commercial vendors and were used without any further purification.

General Procedure for the Synthesis of 5-Substituted-1H-tetrazoles **3 (Table 2).** To a solution of TMSCl (19 μ L, 0.15 mmol) in NMP (1 mL) were added NaN₃ (65 mg, 1.2 mmol) and the corresponding nitrile (1 mmol). The reaction mixture was stirred for 1 min and was subsequently irradiated in a single-mode microwave instrument (Biotage Initiator 2.5) at 220 °C for 15–25 min (see Table 2). Workup A: The reaction mixture was poured into 10 mL of H₂O. The pH of the solution was adjusted to ~pH 1 with concentrated HCl (Caution: gas evolution). The mixture was cooled in an ice-bath, and the precipitate was collected by filtration and washed thoroughly with cold 1 N HCl to furnish the desired tetrazole. Workup B: The reaction mixture was poured into 10 mL of saturated NaHCO₃ and extracted three times with 20 mL of CHCl₃. The aqueous phase was carefully acidified with concentrated HCl to ~pH 1 (Caution: gas evolution) and extracted three times with 20 mL of EtOAc. The combined organic phases were dried over magnesium sulfate and concentrated in vacuo to obtain the pure tetrazole products.

Caution: Hydrazoic acid and its salts are highly poisonous compounds, and hydrazoic acid itself and many of its heavy metal salts explode easily without obvious reasons. Proper protective measures (proper shielding and an additional safety screen in the fume hood, safety glasses or a face shield, leather coat, leather or Kevlar gloves) should be used when undertaking work involving NaN₃/HN₃.

5-Phenyltetrazole (3a). Workup A was used, mp 217–218 °C, lit.^{5b} mp 215–215 °C with decomp.; ¹H NMR (300 MHz, DMSO-*d*₆) δ 7.59–7.65 (m, 3H, aromatic), 8.03–8.06 (m, 2H, aromatic), 16.31 (s, 1H, NH).

5-(4'-Tolyl)tetrazole (3b). Workup A was used, mp. 251–252 °C, lit.^{5f} mp 246–248 °C with decomp.; ¹H NMR (300 MHz, DMSO-*d*₆) δ 7.93 (d, *J* = 8.0 Hz, 2H, aromatic), 7.41 (d, *J* = 8.0 Hz, 2H, aromatic), 2.38 (s, 3H, CH₃).

5-(4'-Chlorophenyl)tetrazole (3c). Workup A was used, mp 252–254 °C with decomp., lit.^{5f} mp 252–254 °C; ¹H NMR (300 MHz, DMSO-*d*₆) δ 8.05 (d, *J* = 8.4 Hz, 2H, aromatic), 7.69 (d, *J* = 8.4 Hz, 2H, aromatic).

5-(4'-(Trifluoromethyl)phenyl)tetrazole (3d). Workup A was used, mp 222–223 °C with decomp., lit.^{5f} mp 221–222 °C; ¹H NMR (300 MHz, DMSO-*d*₆) δ 8.26 (d, *J* = 8.1 Hz, 2H, aromatic), 7.98 (d, *J* = 8.1 Hz, 2H, aromatic).

5-(3'-Methoxyphenyl)tetrazole (3e). Workup A was used, mp 158–160 °C, lit.^{5c} mp 156–157 °C; ¹H NMR (300 MHz, DMSO-*d*₆) δ 7.59–7.64 (m, 2H, aromatic), 7.52 (t, *J* = 8.0 Hz, 1H, aromatic), 7.16 (dd, *J* = 2.4 and 8.1 Hz, 1H, aromatic), 3.85 (s, 3H, CH₃).

5-(3'-Nitrophenyl)tetrazole (3f). Workup A was used, mp 118–120 °C with decomp., lit.²⁵ mp 145–146 °C; ¹H NMR (300 MHz, DMSO-*d*₆) δ 8.82 (s, 1H, aromatic), 8.40–8.47 (m, 2H, aromatic), 7.90 (t, *J* = 8.1 Hz, 1H, aromatic).

5-Benzyltetrazole (3g). Workup B was used, mp 123–124 °C, lit.^{5c} mp 121–122 °C; ¹H NMR (300 MHz, DMSO-*d*₆) δ 7.34–7.36 (m, 2H, aromatic), 7.26–7.28 (m, 3H, aromatic), 4.29 (s, 2H, CH₂).

5-((4'-Chlorophenyl)methyl)tetrazole (3h). Workup B was used, mp 160–162 °C, lit.²⁶ mp 164 °C; ¹H NMR (300 MHz, DMSO-*d*₆) δ 7.40 (d, *J* = 8.4 Hz, 2H, aromatic), 7.30 (d, *J* = 8.4 Hz, 2H, aromatic), 4.30 (s, 2H, CH₂).

5-(2'-Furyl)tetrazole (3i). Workup B was used, mp 201–203 °C, lit.^{5c} mp 204–205 °C; ¹H NMR (300 MHz, DMSO-*d*₆) δ 8.06 (m, 1H, CH), 7.29 (d, *J* = 3.6 Hz, 1H, CH), 6.79–6.81 (m, 1H, CH).

ASSOCIATED CONTENT

S Supporting Information. Complete ref 13, C–N bond length scans for formation of intermediates **22** and **33**, supplementary figures, Cartesian coordinates, energy, and imaginary frequency (transition states) for all the calculated stationary points. This material is available free of charge via the Internet at <http://pubs.acs.org>.

AUTHOR INFORMATION

Corresponding Author

oliver.kappe@uni-graz.at

Present Addresses

[†]Departamento de Química Orgánica e Inorgánica, QUOREX Research Group, Facultad de Ciencias, Universidad de Extremadura, E-06006 Badajoz, Spain.

ACKNOWLEDGMENT

This work was supported by a grant from the Christian Doppler Research Society (CDG). D.C. thanks the Spanish Ministerio de Educación y Ciencia for a fellowship and the Research, Technological Innovation, and Supercomputing Center of Extremadura (CénitS) for their support in the use of LUSITANIA computer resources.

REFERENCES

- (1) (a) Herr, R. J. *Bioorg. Med. Chem.* **2002**, *10*, 3379–3393. (b) Myznikov, L. V.; Hrabalek, A.; Koldobskii, G. I. *Chem. Heterocycl. Compd.* **2007**, *43*, 1–9.
- (2) (a) Wittenberger, S. J. *Org. Prep. Proced. Int.* **1994**, *26*, 499–531. (b) Butler, R. N. In *Comprehensive Heterocyclic Chemistry II*; Katritzky, A. R., Rees, C. W., Scriven, E. F. V., Eds.; Pergamon: Oxford, 1996; Vol. 4, p 621. (c) Gaponik, P. N.; Voitekhovich, S. V.; Ivashkevich, O. A. *Russ. Chem. Rev.* **2006**, *75*, 507–539.
- (3) (a) Finnegan, W. G.; Henry, R. A.; Lofquist, R. J. *Am. Chem. Soc.* **1958**, *80*, 3908–3911. (b) Herbst, R. M.; Wilson, K. R. *J. Org. Chem.* **1957**, *22*, 1142–1145. (c) Mihina, J. S.; Herbst, R. M. *J. Org. Chem.* **1950**, *15*, 1082–1092. (d) Kumar, A.; Narayanan, R.; Shechter, H. *J. Org. Chem.* **1996**, *61*, 4462–4465. (e) Venkateshwarlu, G.; Premalatha, A.; Rajanna, K. C.; Saiprakash, P. K. *Synth. Commun.* **2009**, *39*, 4479–4485. (f) Venkateshwarlu, G.; Rajanna, K. C.; Saiprakash, P. K. *Synth. Commun.* **2009**, *39*, 426–432.
- (4) (a) Kantam, M. L.; Kumar, K. B. S.; Raja, K. P. *J. Mol. Catal. A: Chem.* **2006**, *247*, 186–188. (b) Kantam, M. L.; Balasubrahmanyam, V.; Kumar, K. B. S. *Synth. Commun.* **2006**, *36*, 1809–1814. (c) Nasrollahzadeh, M.; Bayat, Y.; Habibi, D.; Moshaei, S. *Tetrahedron Lett.* **2009**, *50*, 4435–4438. (d) He, J.; Li, B.; Chen, F.; Xu, Z.; Yin, G. *J. Mol. Catal. A: Chem.* **2009**, *304*, 135–138. (e) Das, B.; Reddy, C. R.; Kumar, D. N.; Krishnaiah, M.; Narender, R. *Synlett* **2010**, 391–393.
- (5) (a) Huff, B. E.; Staszak, M. A. *Tetrahedron Lett.* **1993**, *34*, 8011–8014. (b) Demko, Z. P.; Sharpless, K. B. *Org. Lett.* **2001**, *3*, 4091–4094. (c) Amantini, D.; Belaggia, R.; Fringuelli, F.; Pizzo, F.; Vaccaro, L. *J. Org. Chem.* **2004**, *69*, 2896–2898. (d) Bliznets, I. V.; Vasil'ev, A. A.; Shorshnev, S. V.; Stepanov, A. E.; Lukyanov, S. M. *Tetrahedron Lett.* **2004**, *45*, 2571–2573. (e) Jin, T.; Kitahara, F.; Kamijo, F.; Yamamoto, Y. *Tetrahedron Lett.* **2008**, *49*, 2824–2827. (f) Bonnamour, J.; Bolm, C. *Chem.-Eur. J.* **2009**, *15*, 4543–4545.
- (6) (a) McMurray, J. S.; Khabashesku, O.; Britwistle, J. S.; Wang, W. *Tetrahedron Lett.* **2000**, *41*, 6555–6558. (b) Rival, Y.; Wermuth, C. G. *Synth. Commun.* **2000**, *30*, 1587–1591. (c) Duncia, J. V.; Pierce, M. E.; Santella, J. B. *J. Org. Chem.* **1991**, *56*, 2395–2400. (d) Curran, D. P.; Hadida, S.; Kim, S.-Y. *Tetrahedron* **1999**, *55*, 8997–9006.
- (7) (a) Arnold, C.; Thatcher, D. N. *J. Org. Chem.* **1969**, *34*, 1141–1142. (b) Aureggi, V.; Sedelmeier, G. *Angew. Chem., Int. Ed.* **2007**, *46*, 8440–8444.
- (8) (a) Demko, Z. P.; Sharpless, K. B. *J. Org. Chem.* **2001**, *66*, 7945–7950. (b) Himo, F.; Demko, Z. P.; Noodleman, L.; Sharpless, K. B. *J. Am. Chem. Soc.* **2003**, *125*, 9983–9987. (c) Shie, J.-J.; Fang, J.-M. *J. Org. Chem.* **2003**, *68*, 1158–1160. (d) Myznikov, L. V.; Roh, J.; Artamonova, T. V.; Hrabalek, A.; Koldobskii, G. I. *Russ. J. Org. Chem.* **2007**, *43*, 765–767. (e) Zhu, Y.; Ren, Y.; Cai, C. *Helv. Chim. Acta* **2009**, *92*, 171–175.
- (9) (a) Jursic, B. S.; Zdravkovsky, Z. *THEOCHEM* **1994**, *312*, 11–22. (b) Chen, C. *Int. J. Quantum Chem.* **2000**, *80*, 27–37. (c) Himo, F.; Demko, Z. P.; Noodleman, L.; Sharpless, K. B. *J. Am. Chem. Soc.* **2002**, *124*, 12210–12216.
- (10) Himo, F.; Demko, Z. P.; Noodleman, L.; Sharpless, K. B. *J. Am. Chem. Soc.* **2003**, *125*, 9983–9987.
- (11) (a) Wittenberger, S. J.; Donner, B. G. *J. Org. Chem.* **1993**, *58*, 4139–4141. (b) Bliznetsa, I. V.; Vasil'ev, A. A.; Shorshnev, S. V.; Stepanova, A. E.; Lukyanov, S. M. *Tetrahedron Lett.* **2004**, *45*, 2571–2573. (c) Schulz, M. J.; Coats, S. J.; Hlasta, D. J. *Org. Lett.* **2004**, *6*, 3265–3268.
- (12) (a) Dalko, P. I.; Moisan, L. *Angew. Chem., Int. Ed.* **2004**, *43*, 5138–5175. (b) A special issue of Chemical Review about organocatalysis has been published (*Chem. Rev.* **2007**, *107*, 5314–5883).
- (13) Frisch, M. J.; et al. *Gaussian 09*, revision A.1; Gaussian, Inc.: Wallingford, CT, 2009.
- (14) (a) Becke, A. D. *J. Chem. Phys.* **1993**, *98*, 5648–5652. (b) Lee, C.; Yang, W.; Parr, R. G. *Phys. Rev. B* **1988**, *37*, 785–789.
- (15) Zhao, Y.; Truhlar, D. G. *Theor. Chem. Acc.* **2008**, *120*, 215–241.
- (16) Zhao, Y.; Truhlar, D. G. *Acc. Chem. Res.* **2008**, *41*, 157–167.
- (17) Andrae, D.; Häusserman, U.; Dolg, M.; Stoll, H.; Preuss, H. *Theor. Chim. Acta* **1990**, *77*, 123–141.
- (18) Huzinaga, S.; Anzelm, J.; Klubukowski, M.; Radzio-Andzelm, E.; Sakai, Y.; Tatewaki, H. *Gaussian Basis Sets for Molecular Calculations*; Elsevier: Amsterdam, 1984.
- (19) Marenich, A. V.; Cramer, C. J.; Truhlar, D. G. *J. Phys. Chem. B* **2009**, *113*, 6378–6396.
- (20) The conformational flexibility caused by *n*-butyl groups in the dialkyltin oxide reagent used experimentally is minimized by incorporating methyl groups instead.
- (21) Bassindale, A. R.; Stout, T. *Tetrahedron Lett.* **1985**, *26*, 3403–3406 and references therein.
- (22) Smith, D. C.; Lee, S. W.; Fuchs, P. L. *J. Org. Chem.* **1994**, *59*, 348–354.
- (23) Breitenmoser, R. A.; Heimgartner, H. *Helv. Chim. Acta* **2002**, *85*, 885–912.
- (24) Gutmann, B.; Roduit, J.-P.; Roberge, D.; Kappe, C. O. *Angew. Chem., Int. Ed.* **2010**, *49*, 7101–7105.
- (25) Jursic, B. S.; LeBlanc, B. W. *J. Heterocycl. Chem.* **1998**, *35*, 405–408.
- (26) Wehman, T. C.; Popov, A. I. *J. Phys. Chem.* **1966**, *70*, 3688–3693.